

Histological and Immunohistochemical Study on the Effect of Bosutinib on the Lung of Adult Male Albino Rats and the Possible Ameliorating Effect of N-acetyl Cysteine

Amira Fahmy Ali and Nadia said badawy khair

Department of Histology, Faculty of Medicine; Menoufia University, Egypt

ABSTRACT

Background: Bosutinib is in a group of medications named tyrosine kinase inhibitors and is utilized to treat definite type of chronic myeloid leukemia. It might inhibit an abnormal protein that stimulates cancer cells to proliferate. bosutinib administration have some respiratory complications. N- acetylcysteine (NAC) is drug that could be utilized to treat conditions as cystic fibrosis and asthma. NAC is a byproduct of glutathione.

Objective: The target of this work is to estimate the impact of bosutinib, on the rat's lung and the potential protective effect of NAC.

Materials and Methods: This study was carried on forty-eight adults male rats. They were divided into control group, NAC treated group, bosutinib treated group and finally, bosutinib and NAC treated group. At the end of experiment, the lung tissues were processed for biochemical, histological and immunohistochemical studies.

Results: Bosutinib treated group revealed variable degree of histological alterations. Some alveoli appeared collapsed with presence of hyaline material deposition in others, they were mainly lined by type II pneumocytes. The inter-alveolar septa were thick. Cellular infiltration and congested blood vessels with perivascular fibrosis were noticed. Ultrastructurally, type I and type II pneumocytes exhibited degenerative changes. Biochemical results revealed marked increase in the malondialdehyde (MDA) and a marked decrease in the superoxide dismutase (SOD) and glutathione (GSH) levels. These changes were less evident by co-administration of NAC.

Conclusion: Bosutinib has a toxic effect on the lung tissue which could be ameliorated by coadministration of NAC.

Received: 11 January 2021, **Accepted:** 06 March 2021

Key Words: α -SMA, bosutinib, caspase-3, iNOS, lung, NAC.

Corresponding Author: Amira Fahmy Ali, MD, Department of Histology, Faculty of Medicine; Menoufia University, Egypt, **Tel.:** +20 10689 15402, **E-mail:** amirafahmy356@yahoo.com

ISSN: 1110-0559, Vol. 45, No.1

INTRODUCTION

Tyrosine kinase inhibitors (TKIs) is a group of chemotherapy medications which block one or more of the enzyme tyrosine kinases. More than twenty types of TKIs were approved by Food and Drug Administration (FDA) in 2018^[1]. Tyrosine kinases are cell membrane receptors, called molecular structures that send and receive signals from the environment^[2]. Various multi-targeted kinase inhibitors have been confirmed for treatment of several tumor types and, they persist to be of benefit in pharmaceutical field^[3].

Chronic myeloid leukemia (CML) is associated cytogenetically with the existence of the Philadelphia chromosome that appeared as a result of a chromosomal translocation between the Abelson (Abl) gene on chromosome 9 and the breakpoint cluster region (BCR) on chromosome 22, leading to the constitutively active BCR-Abl tyrosine kinase which enhances myeloid proliferation in CML^[4]. The most important cellular target for TKIs have been the BCR-Abl, which is the responsible protein for the cancer types; chronic myeloid leukemia and acute lymphoblastic leukemia^[5]. However, potentially serious

lung complications of TKIs as interstitial lung disease, pulmonary arterial hypertension and pleural effusions were reported^[6].

Bosutinib (Bosulif) is a small molecule, multi-targeted kinase inhibitor^[7]. It is a new second-generation TKI, confirmed for patients with CML which is resistant to dasatinib, nilotinib or imatinib^[8]. It works by inhibiting various forms of BCR-ABL kinase which promotes CML. In lab rat cells, Bosulif was shown to inhibit 16 of 18 forms of BCR-ABL kinase that were resistant to imatinib^[9]. Though the most common side effects of bosutinib are gastrointestinal, long-term bosutinib studies have reported respiratory complications. Pleural effusion has been determined in CML treated with bosutinib, with an overall incidence of 7-9%^[10].

N - acetylcysteine (NAC) is a dietary complement obtained from L-cysteine, amino acid. It is naturally present in garlic, red peppers, broccoli, onions and soya seeds. It is also found in whole grain products as cereals and bread^[11]. It is used as an antidote for overdose of paracetamol and to dissolve thick mucus in patients with chronic respiratory disorders as bronchitis and pneumonia^[12]. NAC is known

for its hepatoprotective characteristic and to assist healthy immune function^[13]. NAC is a precursor to glutathione (GSH) where in the body, NAC is converted to cysteine which in turn is converted into glutathione. Glutathione is a tri-peptide that fights free radicals which causes cell damage^[14]. NAC has been suggested for use in the prevention and treatment of various respiratory diseases and of diseases including an oxidative stress involving COVID-19^[15].

Data on the effect of bosutinib on the lung structure was very scarce. So, this study pointed to estimate the potential effects of the novel TKI bosutinib, on the histological structure of the rat's lung and to impact the protective effect of NAC using histological and immunohistochemical studies.

MATERIALS AND METHODS

Forty-eight adult male albino rats were utilized in the current work. Their weights ranged between 150 to 200 gm. Animals were housed in metal cages at suitable constant temperature and were exposed to day light from 10-12 hours. The rats were allowed free access to food and water. Strict hygiene was followed to keep a healthy medium. Animal treatment was according to ethical protocol that was confirmed by the Ethical Committee of Menoufia University, Faculty of Medicine, Egypt.

Experimental procedure

The animals were separated randomly into four groups, 12 animals each:

Group I (control group): animals were left untreated and provided an ordinary diet.

Group II (NAC treated group): Animals received NAC (200mg sachets, SEDICO Pharmaceutical company, each sachet was dissolved in 30ml water) at a dose of 50 mg/kg by gavage once a day for 8 weeks^[16]. Each animal received 1.4 ml.

Group III (bosutinib treated group): Animals received bosutinib (bosulif, 500mg tablets, Pfizer company, each tablet was dissolved in 30ml distilled water) at a dose of 50 mg/kg/day by gavage, once a day for 8 weeks^[17]. Each animal received 0.5ml.

Group IV (bosutinib and NAC treated group): Animals received bosutinib and NAC simultaneously in the same doses and route of administration as groups II and III for 8 weeks.

At the appropriate time, Ketamine (90mg/kg)^[18] was injected intraperitoneally to anaesthetize the rats from all groups. The chest cavity was opened. The right and left lungs were carefully obtained and processed for biochemical, histological and immunohistochemical studies.

1-Biochemical study

For determination of the oxidant and antioxidant enzymes, the right lung tissues were removed and

homogenized in PBS and then, centrifuged at 4500 rpm for 15 min, the supernatant was obtained for assessment of malondialdehyde (MDA)^[19], glutathione (GSH)^[20] and superoxide dismutase (SOD) levels^[21], employing a spectrophotometer.

II-Histological study

A-Light microscopic study

Right lung specimens were fixed in formal saline, washed and processed to obtain paraffin sections, 5 µm in thickness. Then, sections were stained via hematoxylin and eosin (Hx& E) to point out the histological structure and Mallory's trichrome stain to detect the collagen fibers^[22].

B-Electron microscopic study

Left lung pieces were fixed in 2.5 percent glutaraldehyde for 1 hour for transmission electron microscope (TEM) analysis. Post fixed in osmium tetroxide and then incubated in uranyl acetate and embedded in Epon, sections were obtained and, stained via 1 % toluidine blue then ultrathin sections were obtained. The sections were examined and photographed using a Jeol- JEM- 100 CXII (Joel, Tokyo, Japan)^[23]. TEM processing and analysis were done at the Unit of Electron Microscopy, Faculty of Medicine, Tanta University.

III-Immunohistochemical study

Immunohistochemical staining was performed using polyclonal rabbit antibodies for anti-cleaved Caspase 3 (PA1-26426), anti-inducible nitric oxide synthase (PA1-036) (iNOS) while monoclonal antibodies were used for anti-alpha smooth muscle actin (α -SMA) (Sigma-Aldrich, St. Louis, MO, USA). Sections were deparaffinized, hydrated, washed in 0.1M phosphate buffer saline (PBS). Endogenous peroxidases were blocked by treatment with H₂O₂ in methanol (Peroxidase blocking solution) followed by washing in tri buffer saline (TBS). Then sections were incubated with diluted primary antibodies for iNOS (1:100), Caspase 3 (1:200) and α -SMA (1:100). Sections then washed three times each for 5 minutes in buffer and incubated for further 30 minutes with biotinylated goat anti-rabbit secondary antibodies diluted 1:1000, followed by washing. Following further 30 minutes incubation with Vectastain ABC kits (Avidin, Biotinylated horse radish peroxidase Complex) and washing for 10 minutes. Diaminobenzidine tetra hydrochloride (DAB) in distilled water was added for 5-10 min. Finally, the slides were counterstained by Mayer's hematoxylin, dehydrated in ascending concentrations of alcohol and cleared by xylene. Negative controls were performed by the same steps of immunostaining but the primary antibodies were removed. Tonsils were used a positive control for activated Caspase-3. Lung tissue is considered positive control for iNOS while human uterine leiomyoma served as positive controls for α -SMA according to the company instructions^[24].

IV-Morphometric study and Statistical analysis

All quantitative information was gained utilizing "Leica Qwin 500 C" image analyzer automatic data processing system Ltd. (Cambridge, England). At magnification of 400, in Hx&E stained sections, ten- non overlapping fields taken from 10 slides of every rat within the studied groups were used randomly for assessment of type II pneumocytes number and interalveolar septa thickness, collagen fibers area percentage (%) in Mallory's trichrome stained sections. while the intensity of iNOS, Caspase-3 and α -SMA immunostaining were measured in immunostained sections.

The biochemical and histomorphometric results were analyzed and compared by student's t-test. *P-value* was used to test the significant change in each parameter in the experimental animals in comparison with control group. The data collected were tabulated as mean \pm SD and analyzed using statistical package for the Social Science Software (SPSS) software (version 17.0 on an IBM compatible computer; SPSS Inc., Chicago, Illinois, USA). *P value* was set at 0.05, $P>0.05$ non-significant, $P\text{-value}<0.05$ significant and $P\text{-value}<0.001$ highly significant^[25].

RESULTS

I- Biochemical results

Shown in (Table 1), group II (NAC-treated group) demonstrated a non-significant changes in the levels of MDA (lipid peroxidation marker), GSH and SOD (antioxidant enzymes) in comparison with control animals ($P>0.05$). Group III (bosutinib treated group) displayed a highly significant increase in the level of MDA ($P<0.001$) and a significant decrease in the levels of GSH and SOD ($P<0.05$) in comparison with the animals of control group. Moreover, group IV (bosutinib and NAC- treated group) exhibited a non- significant changes in the mean values of MDA, GSH and SOD ($P>0.05$) when compared with the control animals, while revealed a highly significant decrease in the level of MDA ($P<0.001$) and also, significant increase in the level of antioxidant enzymes ($P<0.05$) when compared with bosutinib treated group (Histograms 1a,1b,1c).

II-Histological results

A-Light microscopic results

Hx&E stained sections of the lung tissue of control groups (groups I&II) were the same and revealed normal histological alveolar structure. There were alveoli, alveolar sacs, alveolar duct, bronchiole and blood vessel (Figure 1). The alveoli were separated by thin inter-alveolar septa and lined by two types of cells. Type I pneumocytes, flattened squamous cells, forming main alveolar lining and type II pneumocytes which were cuboidal in shape. Normal bronchiolar epithelium was seen (Figure 2).

Group III (bosutinib treated group) exhibited histological alterations. Collapsed alveoli, hyaline material

deposition in some alveoli and congested blood vessels were present (Figure 3). Disrupted bronchiolar epithelium containing cellular debris in their lumen was also detected (Figures 3,4). Thick inter-alveolar septa were noticed (Figures 3,4,5). There was apparent increase in the type II pneumocytes number lining the alveoli (Figure 4). Cellular infiltration (Figures 4,5), extravasated blood cells (Figure 5) and congested blood vessels with thickening of its wall and perivascular fibrosis were encountered (Figure 6).

Sections of the of group IV (bosutinib and NAC-treated group) showed nearly normal appearance of the alveolar tissue. Apparent decrease in the thickening of inter-alveolar septa was evident, However, areas of cellular infiltrate and hyaline material deposition were still present (Figure 7). The alveoli with wide alveolar spaces, lined by type I pneumocytes and type II pneumocytes were noticed (Figure 8).

Lung sections stained with Mallory's trichrome in control groups (groups I&II) displayed normal distribution of collagen fibers around walls of bronchiole and blood vessel (Figure 9). While group III (bosutinib treated group) appeared with dense collagen fibers deposition around the bronchioles and blood vessels (Figure 10). Moreover, group IV (bosutinib and NAC-treated group) revealed decreased amount of collagen fibers around the bronchiole (Figure 11).

B-Transmission electron microscopic results

Ultra-thin sections of the lung tissue of control rats (groups I&II) exhibited normal alveolar structure, the alveoli were lined by both types of pneumocytes. Blood capillary was noticed in the inter-alveolar septa (Figure 12). Type I pneumocyte revealed elongated euchromatic nucleus surrounded by a thin rim of cytoplasm. Type II pneumocyte displayed rounded euchromatic nucleus and microvillous border. Its cytoplasm contained lamellar bodies with concentric lamellae, rough endoplasmic reticulum cisternae and mitochondria (Figure 13).

An electron microscopic examination of Group III (bosutinib treated group) revealed marked alterations of alveolar architecture. Type I pneumocytes were also seen with irregular heterochromatic nuclei (Figures 14,16) and surrounded by collagen fibers (Figure 14). Eosinophil cell with its characteristic granules within congested blood vessel was seen (Figure 14). Type II pneumocytes containing irregular heterochromatic nuclei, empty lamellar bodies (Figures 14,15,17), swollen mitochondria, blunted microvillous border (Figures 15,17) and rough endoplasmic reticulum cisternae (Figure 17) were observed. Characteristic granules of the eosinophil cell were seen (Figure 17). While an electron microscopic examination of the Group IV (bosutinib and NAC-treated group) revealed preservation of the alveolar tissue. The alveoli were patent and lined by both types of pneumocytes. Type I pneumocyte had elongated euchromatic nucleus, alveolar macrophage with lamellipodia and kidney shaped

nucleus was observed within alveolus (Figure 18). Type II pneumocytes having euchromatic nuclei, multiple lamellar bodies and microvillous border (Figure 19).

III-Immunohistochemical results

Anti-iNOS immune expression of control groups (groups I&II) revealed negative expression in the lung tissue (Figure 20). Group III (bosutinib treated group) displayed obvious positive immunoreaction for iNOS in the cells scattered in the inter-alveolar septa (Figure 21). Moreover, group IV (bosutinib and NAC-treated group) exhibited less obvious positive immunoreaction for iNOS in some cells in the inter-alveolar septa (Figure 22).

Anti-caspase-3 immune-marker expression of control groups (groups I&II) displayed negative immune expression in the lung tissue (Figure 23). Group III (bosutinib treated group) revealed obvious positive cytoplasmic caspase-3 immune expression in the alveolar epithelium and the cells present in the inter-alveolar septa (Figure 24). While group IV (bosutinib and NAC-treated group) revealed minimal positive cytoplasmic caspase-3 immunoreaction in the lung tissue (Figure 25).

Regarding α -SMA immune expression, lung sections of control groups (groups I&II) showed positive immunoreaction in the wall of blood vessel and bronchiole (Figure 26). While group III (bosutinib treated group) revealed markedly increased expression for α -SMA in the wall of blood vessel, bronchial tree and the inter-alveolar septa (Figure 27). Sections of the lung tissue of group IV (bosutinib and NAC treated group) revealed decreased expression for α -SMA in the wall of blood vessel, bronchiole and inter-alveolar septa (Figure 28).

IV-Morphometric and statistical results

Data in (Table 2) demonstrated that group III (bosutinib treated group) exhibited a highly significant increase in the number of type II pneumocytes and inter-alveolar septa thickness ($P<0.001$) when compared with the control animals, while group IV (bosutinib and NAC-treated group) revealed a non-significant change in these parameters ($P>0.05$) when compared with the control animals and a highly significant changes in comparison with bosutinib treated rats (group III) ($P<0.001$) (Histograms 2a,2b).

Data in (Table 3) showed that group III (bosutinib treated group) exhibited a highly significant rise in the mean area % of collagen fibers deposition and mean values of optical density for iNOS and α -SMA ($P<0.001$) and a significant increase in mean optical density for caspase-3 ($P<0.05$) when compared with the control animals. Moreover, group IV (bosutinib and NAC treated group) displayed a non-significant change in the mean area of collagen fibers deposition and the mean optical density for α -SMA ($P>0.05$) and a significant increase in the

mean optical density for iNOS and caspase-3 ($P<0.05$) in comparison with control group (Histograms 3a,3b,3c,3d).

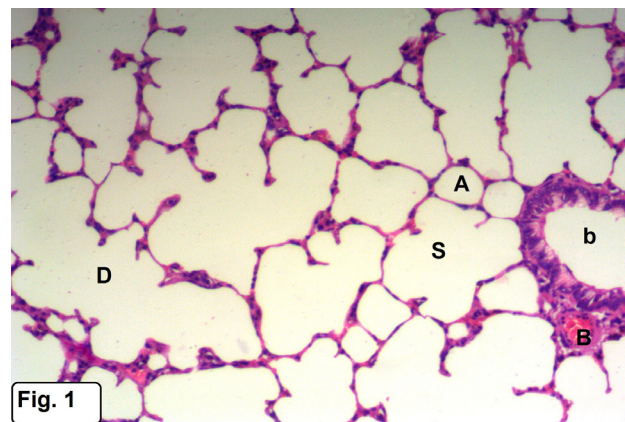


Fig. 1

Fig. 1: A photomicrograph of a section in the lung of group I (control group) illustrating alveoli (A), alveolar sacs (S), alveolar duct (D), bronchiole(b) and blood vessel (B). (Hx&E X100)

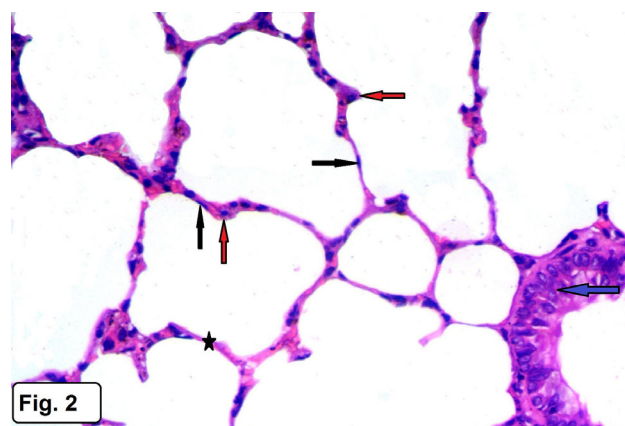


Fig. 2

Fig. 2: A photomicrograph of a section in the lung of group I (control group) showing alveoli with thin inter-alveolar septa (star). The alveoli are lined by type I pneumocytes, flat cells (black arrows) and type II pneumocytes, cuboidal cells (red arrows). Notice, normal bronchiolar epithelium (blue arrow). (Hx&E X200)

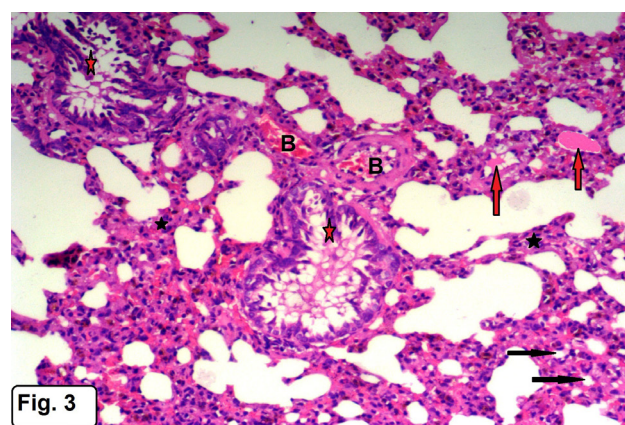


Fig. 3

Fig. 3: A photomicrograph of a section in the lung of group III (bosutinib treated group) showing collapsed alveoli (black arrows), thick inter-alveolar septa (black stars) and congested blood vessels (B). Notice, disrupted bronchiolar epithelium with cellular debris in their lumen (red stars) and hyaline material deposition in some alveoli (red arrows). (Hx&E X100)

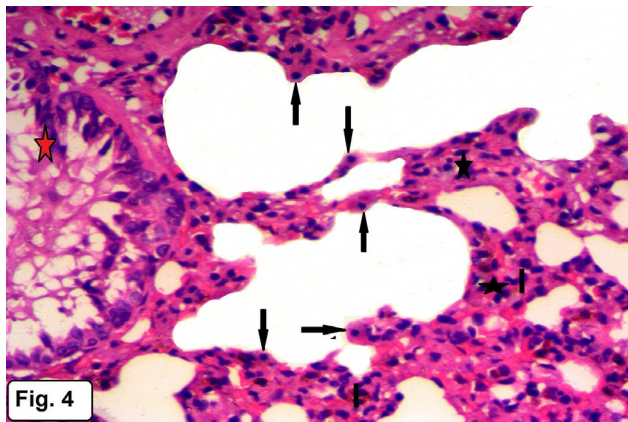


Fig. 4: A photomicrograph of a section in the lung of group III (bosutinib treated group) showing apparent increase in the type II pneumocytes number (arrows) lining the alveoli. Notice, thick inter-alveolar septa (black stars), cellular infiltration (I) and bronchiole with cellular debris in its lumen (red star). (Hx&E X200)

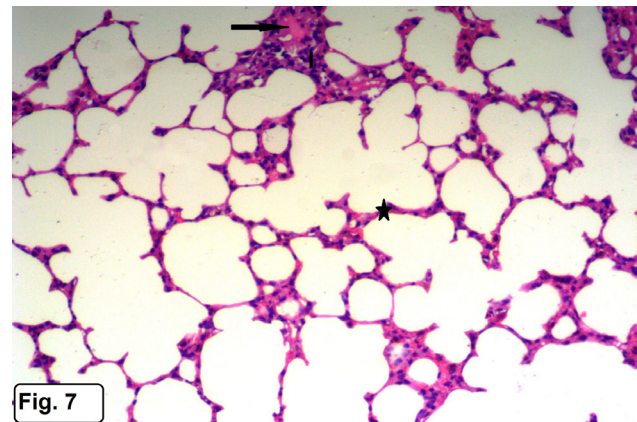


Fig. 7: A photomicrograph of a section in the lung of group IV (bosutinib and NAC treated group) showing apparent decrease in the thickening of inter-alveolar septa (star) with appearance of areas of cellular infiltrate (I) and hyaline material deposition (arrow). (Hx&E X100)

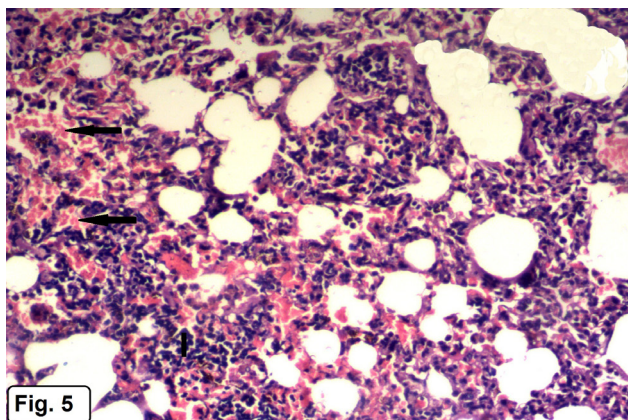


Fig. 5: A photomicrograph of a section in the lung of group III (bosutinib treated group) showing distorted lung architecture, marked inter-alveolar septal thickness, excess cellular infiltration (I) and extravasated blood cells (arrows). (Hx&E X100)

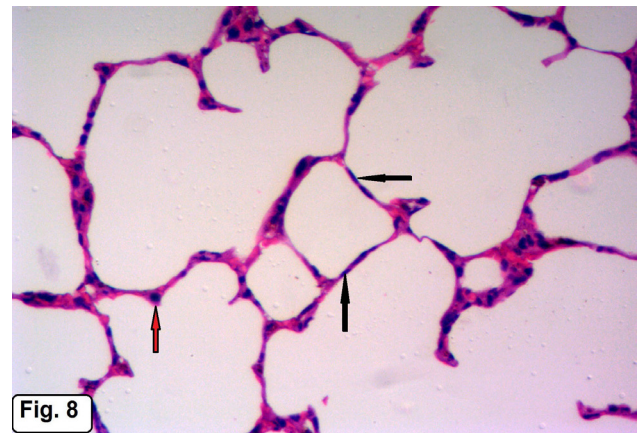


Fig. 8: A photomicrograph of a section in the lung of group IV (bosutinib and NAC treated group) showing alveoli with wide alveolar spaces, lined by type I pneumocytes (black arrows) and type II pneumocytes (red arrow). (Hx&E X200)

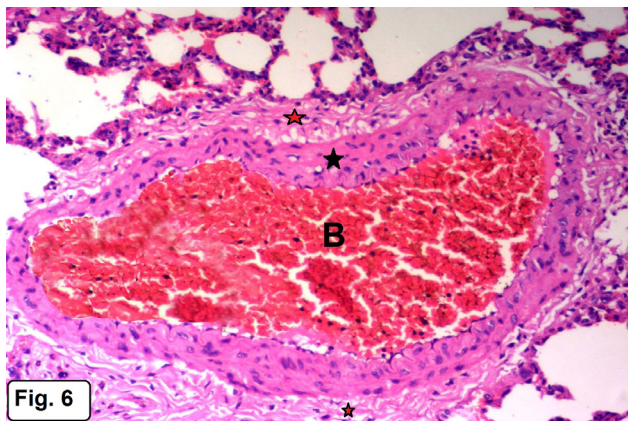


Fig. 6: A photomicrograph of a section in the lung of group III (bosutinib treated group) showing congested blood vessel (B) with thickening of its wall (black star) and perivascular fibrosis (red stars). (Hx&E X100)

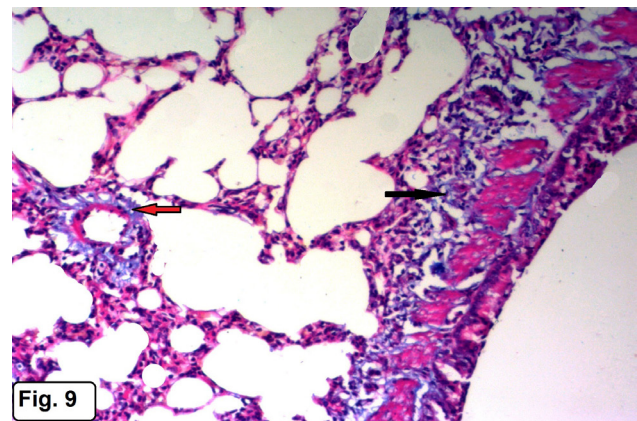


Fig. 9: A photomicrograph of a section in the lung of group I (control group) showing normal distribution of collagen fibers around wall of bronchiole (black arrow) and blood vessel (red arrow). (M.T X100)

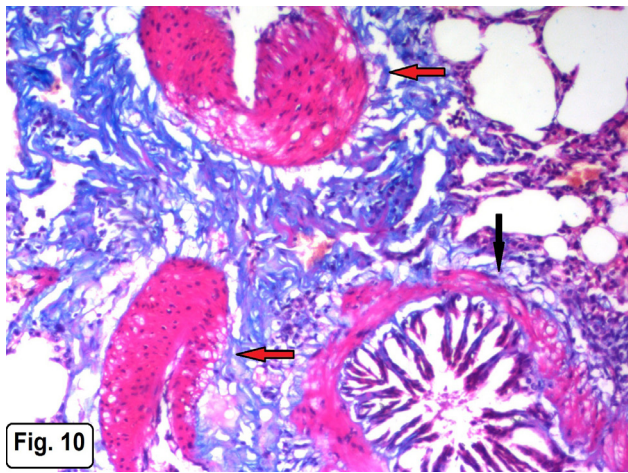


Fig. 10

Fig. 10: A photomicrograph of a section in the lung of group III (bosutinib treated group) showing dense collagen fibers deposition around wall of the bronchiole (black arrow) and blood vessels (red arrows). (M.T X100)

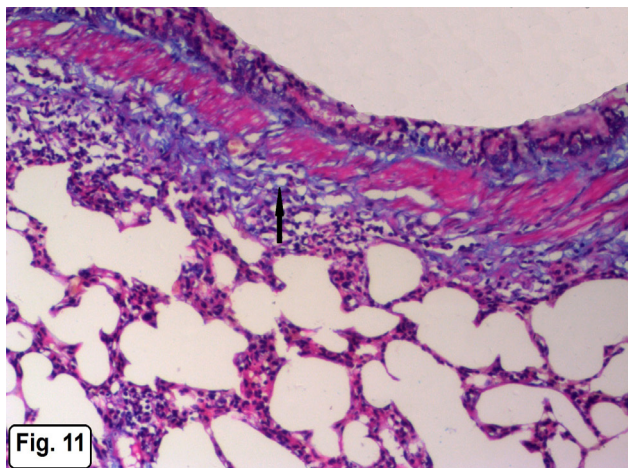


Fig. 11

Fig. 11: A photomicrograph of a section in the lung of group IV (bosutinib and NAC treated group) showing decreased amount of collagen fibers around the wall of the bronchiole (arrow). (M.T X100)

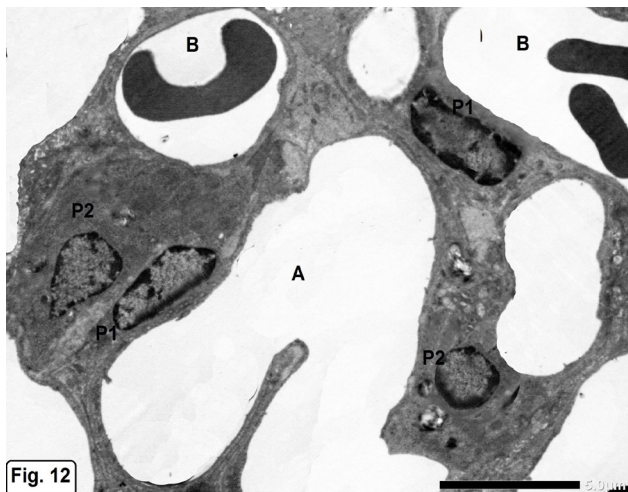


Fig. 12

Fig. 12: An electron micrograph of the lung of group I (control group) showing patent alveoli (A) lined by type I pneumocytes (P1) and type II pneumocyte (P2). Notice, blood capillaries (B). (TEM X1500)

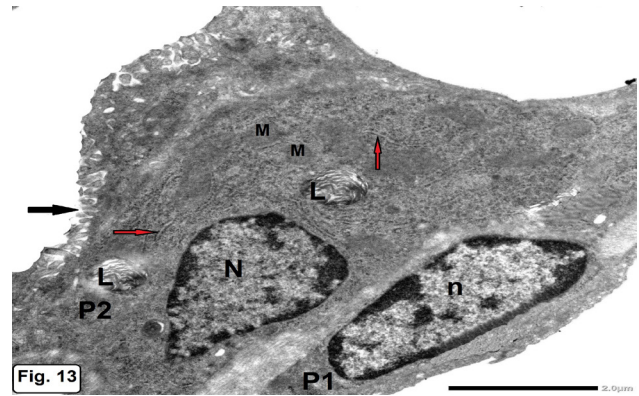


Fig. 13

Fig. 13: An electron micrograph of a section in the lung of group I (control group) showing type I pneumocyte (P1) having elongated euchromatic nucleus (n) surrounded by a thin rim of cytoplasm. Type II pneumocyte (P2) having rounded euchromatic nucleus (N) and microvillous border (black arrow). Its cytoplasm contains lamellar bodies with concentric lamellae (L), mitochondria (M) and rough endoplasmic reticulum cisternae (red arrows). (TEM X4000)

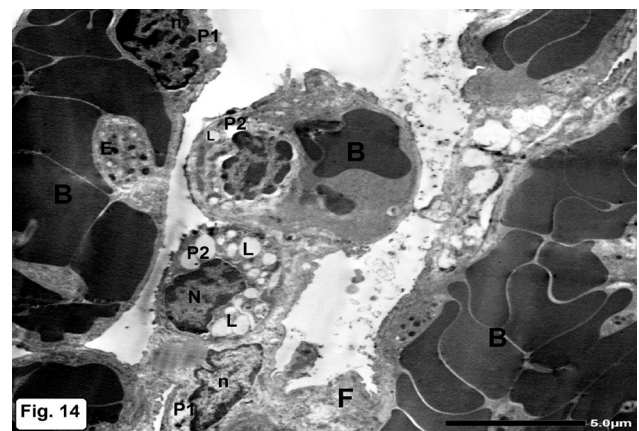


Fig. 14

Fig. 14: An electron micrograph of a section in the lung of group III (bosutinib treated group) showing type I pneumocyte (P1) having irregular nucleus (n) and surrounded by collagen fibers (F). Type II pneumocyte (P2) containing irregular heterochromatic nucleus (N) and multiple empty lamellar bodies (L). Notice, presence of eosinophil cell with its characteristic granules (E) within congested blood capillaries (B). (TEM X1500)

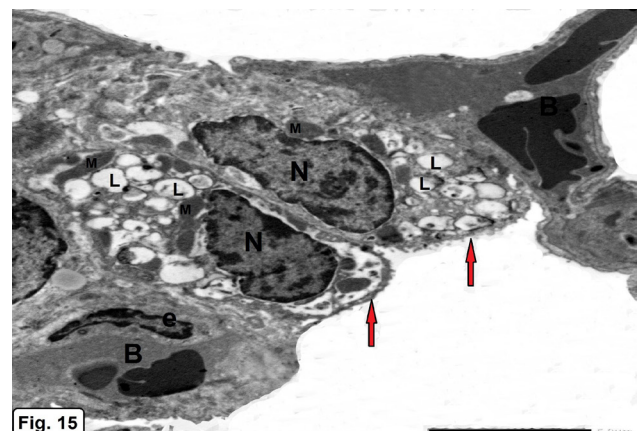


Fig. 15

Fig. 15: An electron micrograph of a section in the lung of group III (bosutinib treated group) showing part of the alveolus (A) lined by type II pneumocyte (P2) having irregular heterochromatic nuclei (N), empty lamellar bodies (L), swollen mitochondria (M) and blunted microvillous border (red arrows). Notice, blood capillaries (B) with endothelial cell (e). (TEM X1500)

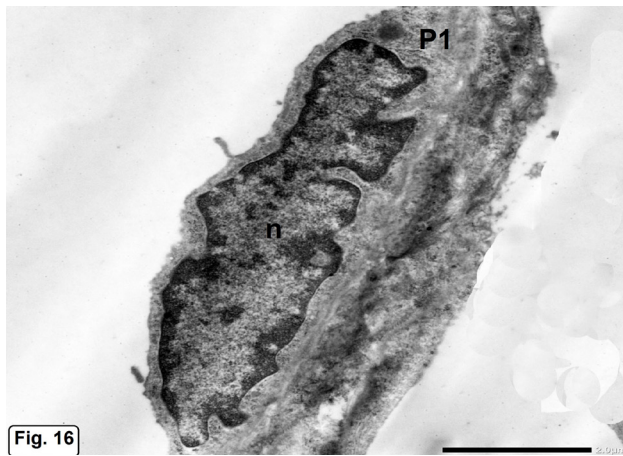


Fig. 16

Fig. 16: An electron micrograph of a section in the lung of group III (bosutinib treated group) showing type I pneumocyte (P1) having irregular heterochromatic nucleus (n). (TEM X4000)

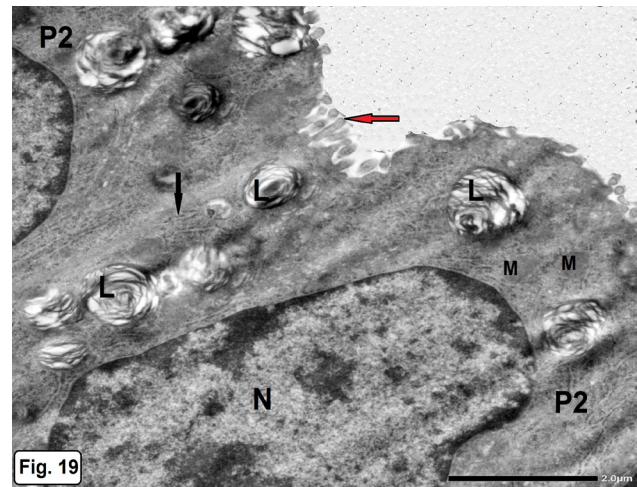


Fig. 19

Fig. 19: An electron micrograph of a section in the lung of group IV (bosutinib and NAC treated group) showing type II pneumocytes (P2) with euchromatic nuclei (N), multiple lamellar bodies (L), mitochondria (M), rough endoplasmic reticulum cisternae (black arrow) and microvillous border (red arrow). (TEM X4000)

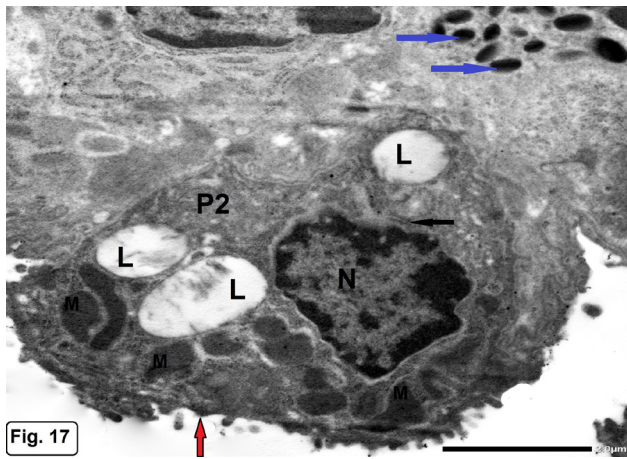


Fig. 17

Fig. 17: An electron micrograph of a section in the lung of group III (bosutinib treated group) showing type II pneumocyte (P2) having irregular heterochromatic nucleus (N), lamellar bodies (L) with loss of characteristic lamellar pattern leaving vacuoles, swollen ballooned mitochondria (M), rough endoplasmic reticulum cisternae (black arrow) and blunted microvillous border (red arrow). Notice, characteristic granules of eosinophil (blue arrows). (TEM X4000)

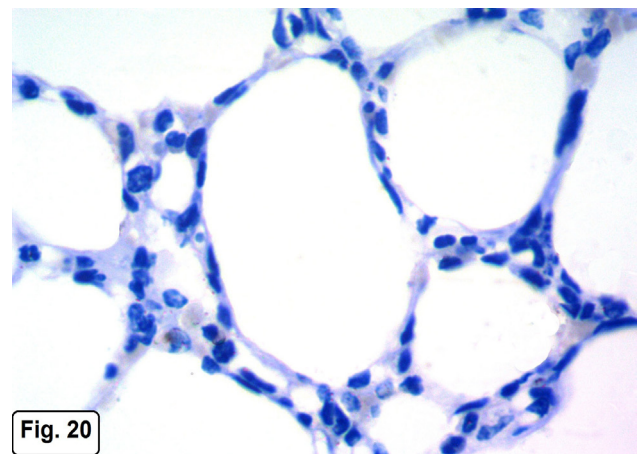


Fig. 20

Fig. 20: A photomicrograph of a section in the lung of group I (control group) showing negative immunoreactions for iNOS in the lung tissue. (iNOS X400)

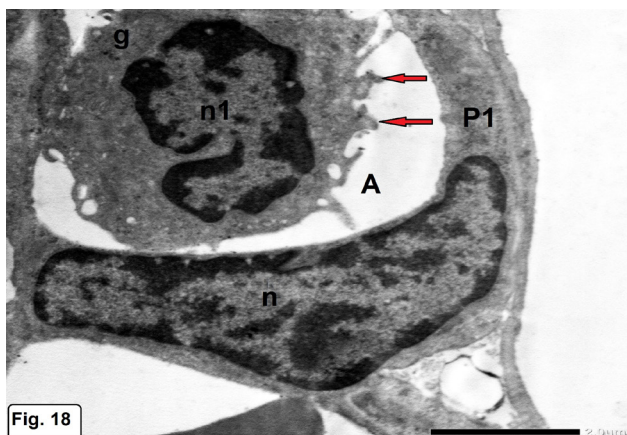


Fig. 18

Fig. 18: An electron micrograph of a section in the lung of group IV (bosutinib and NAC treated group) showing an alveolus (A) lined by type I pneumocyte (P1) appears with elongated euchromatic nucleus (n). Notice, alveolar macrophage (g) with lamellipodia (red arrows) and kidney shaped nucleus (n1). (TEM X4000)

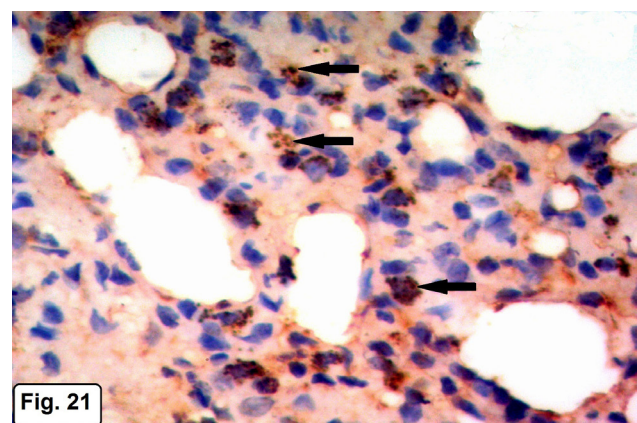


Fig. 21

Fig. 21: A photomicrograph of a section in the lung of group III (bosutinib treated group) showing obvious positive immunoreactions for iNOS in the cells scattered in the inter-alveolar septa (arrows). (iNOS X400)

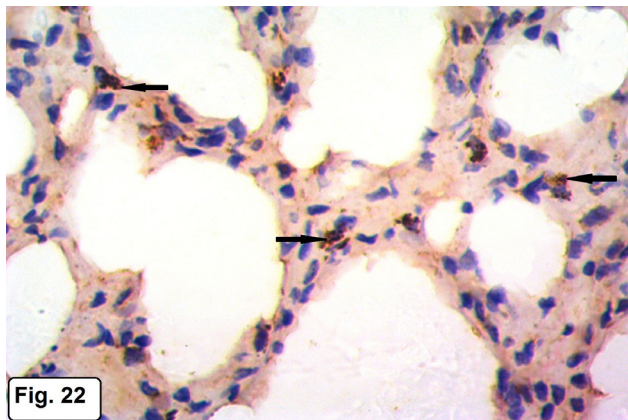


Fig. 22

Fig. 22: A photomicrograph of a section in the lung of group IV (bosutinib and NAC treated group) showing less obvious positive immunoreactions for iNOS in some cells in the inter-alveolar septa (arrows). (iNOS X400)

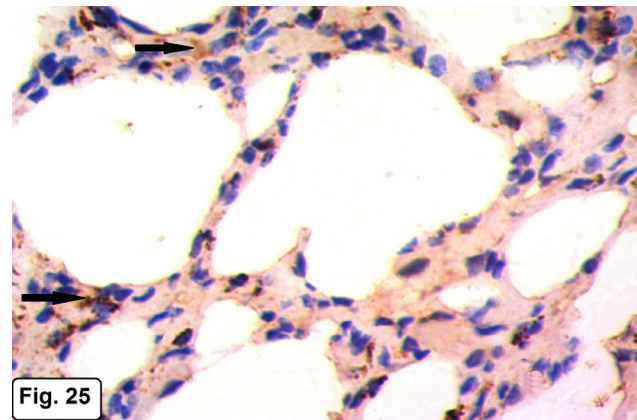


Fig. 25

Fig. 25: A photomicrograph of a section in the lung of group IV (bosutinib and NAC treated group) showing minimal positive caspase-3 immune expression in the cells present in the inter-alveolar septa (arrows). (Caspase-3 X400)

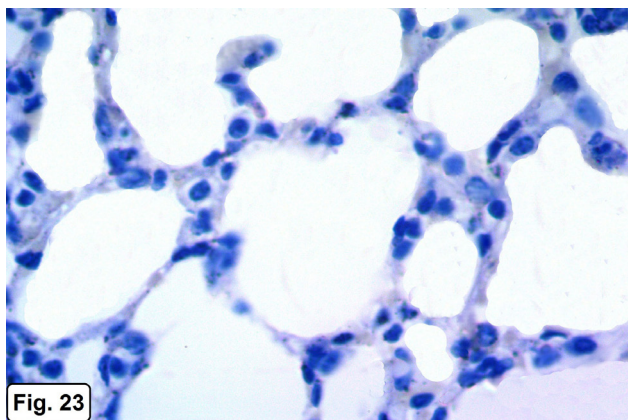


Fig. 23

Fig. 23: A photomicrograph of a section in the lung of group I (control group) showing negative caspase-3 immune expression in the lung tissue. (Caspase-3 X400)

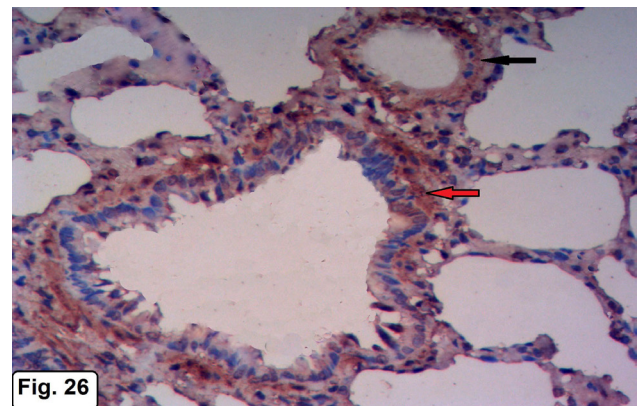


Fig. 26

Fig. 26: A photomicrograph of a section in the lung of group I (control group) showing positive immunoreaction for α -SMA in the wall of blood vessel (black arrow) and bronchiole (red arrow). (α -SMA X200)

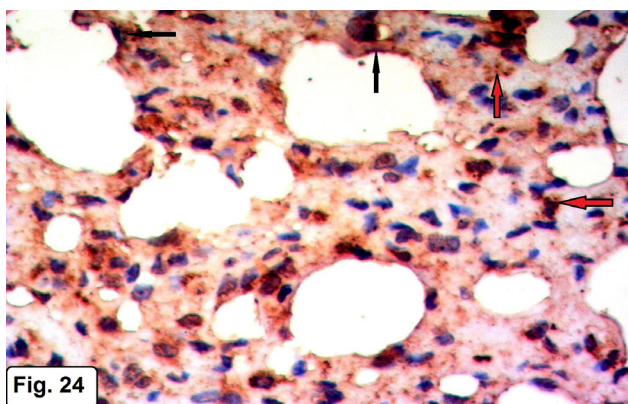


Fig. 24

Fig. 24: A photomicrograph of a section in the lung of group III (bosutinib treated group) showing obvious positive cytoplasmic caspase-3 immune expression in the alveolar epithelium (black arrows) and cells present in the inter-alveolar septa (red arrows). (Caspase-3 X400)

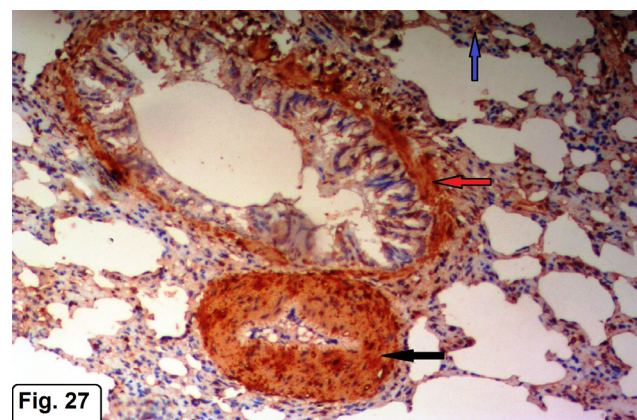


Fig. 27

Fig. 27: A photomicrograph of a section in the lung of group III (bosutinib treated group) showing markedly increased expression for α -SMA in the wall of blood vessel (black arrow), bronchiole (red arrow) and in the inter-alveolar septa (blue arrow). (α -SMA X200)

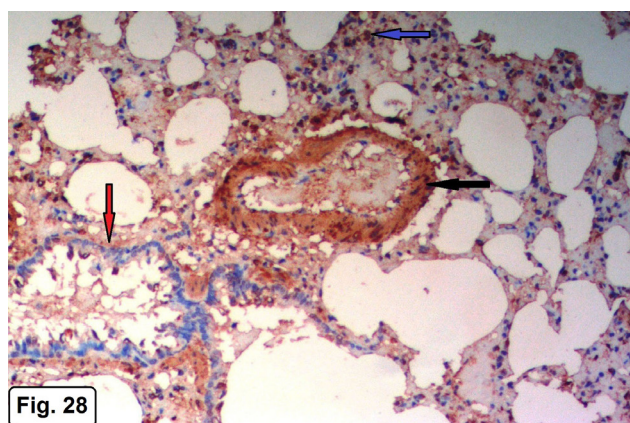


Fig. 28

Fig. 28: A photomicrograph of a section in the lung of group IV (bosutinib and NAC treated group) showing decreased expression for α -SMA in the wall of the blood vessel (black arrow), bronchiole (red arrow) and inter-alveolar septa (blue arrow). (α -SMA X200)

Table 1: Mean values of MDA, GSH and SOD levels in lung tissue in different experimental groups

	Group I M \pm SD	Group II M \pm SD	Group III M \pm SD	Group IV M \pm SD	P value
MDA (nmol/g tissue)	55 \pm 3.3	54.5 \pm 3.1	172.5 \pm 5.3	57.4 \pm 0.3	P1=0.934 P2=0.000 P3=0.367 P4=0.000
GSH (umol/g tissue)	6.8 \pm 0.5	6.6 \pm 0.4	4.8 \pm 1.8	6.3 \pm 0.9	P1=0.285 P2=0.003 P3=0.086 P4=0.035
SOD (U/g)	3.2 \pm 0.4	3 \pm 0.5	2.3 \pm 0.8	2.9 \pm 0.4	P1=0.466 P2=0.006 P3=0.168 P4=0.035

M= the mean value. SD= the standard deviation.

P1 Comparison was done between group II (NAC treated group), and control group

P2 Comparison was done between group III (bosutinib treated group), and control group.

P3 Comparison was done between group IV (bosutinib and NAC treated group), and control group.

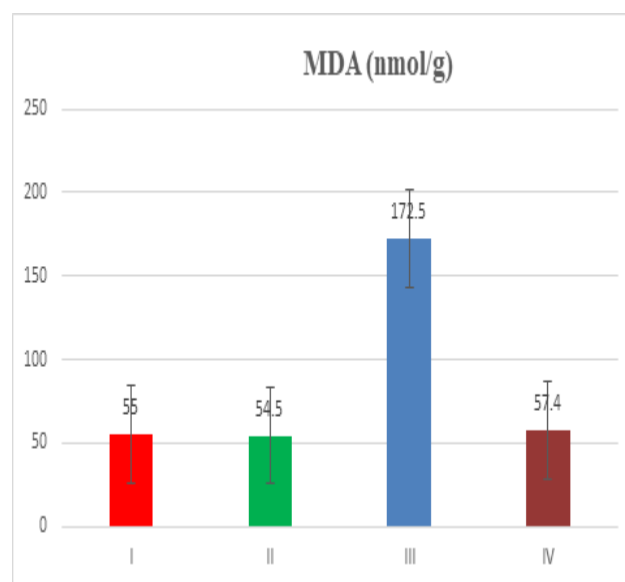
P4 Comparison was done between group IV (bosutinib and NAC treated group) and group III (bosutinib treated group)

Table 2: Mean values of inter-alveolar septa thickness and type II pneumocytes number in different experimental groups

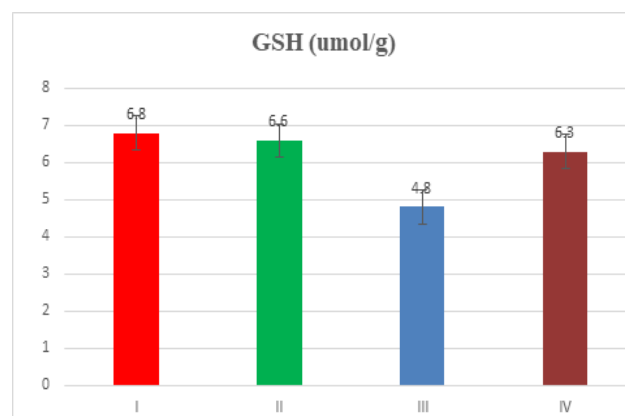
	Group I M \pm SD	Group II M \pm SD	Group III M \pm SD	Group IV M \pm SD	P value
Inter-alveolar septa (μ m)	7.3 \pm 0.5	7.4 \pm 0.6	28 \pm 0.6	7.7 \pm 0.7	P1=0.840 P2=0.000 P3=0.199 P4=0.000
Type II pneumocytes	5.2 \pm 0.6	5 \pm 0.4	10.9 \pm 1.1	4.6 \pm 1	P1=0.420 P2=0.000 P3=0.126 P4=0.000

Table 3: Mean area %of collagen fibers deposition and optical density of iNOS, caspase-3 and α -SMA in different experimental groups

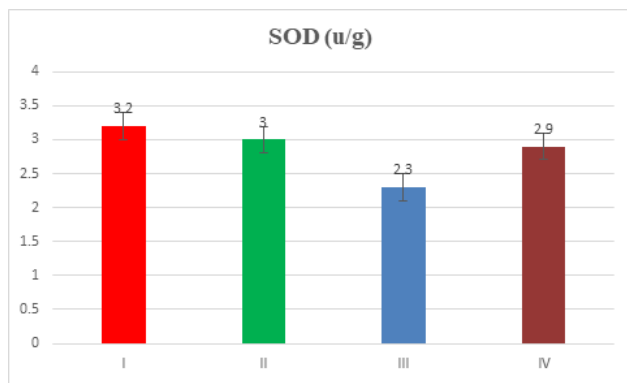
	Group I M \pm SD	Group II M \pm SD	Group III M \pm SD	Group IV M \pm SD	P value
Collagen area %	0.2 \pm 0.0	0.3 \pm 0.2	5.2 \pm 0.8	0.4 \pm 0.3	P1=0.682 P2=0.000 P3=0.077 P4=0.000
iNOS	0.1 \pm 0.1	0.3 \pm 0.1	1.1 \pm 0.5	0.6 \pm 0.5	P1=0.341 P2=0.000 P3=0.006 P4=0.060
Caspase-3	.04 \pm 0.00	0.03 \pm 0.0	0.2 \pm 0.1	0.1 \pm 0.01	P1=0.334 P2=0.003 P3=0.008 P4=0.061
α -SMA	63.3 \pm 1.1	62.5 \pm 1.5	93.9 \pm 3.3	65.6 \pm 3.4	P1=0.188 P2=0.000 P3=0.060 P4=0.000



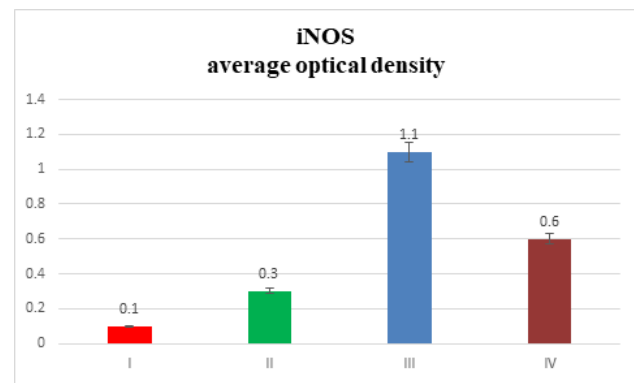
Histogram 1a: Mean values of MDA level in different groups



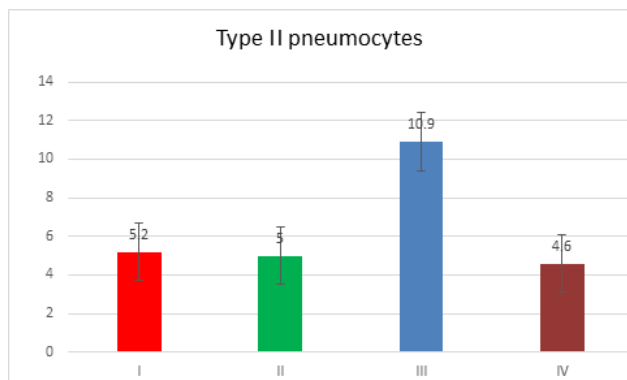
Histogram 1b: Mean values of GSH level in different groups



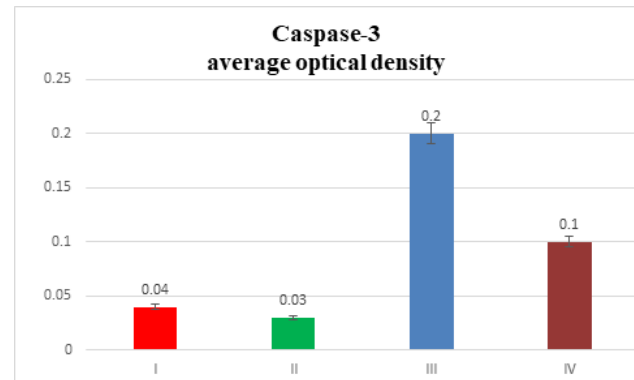
Histogram 1c: Mean values of SOD level in different groups



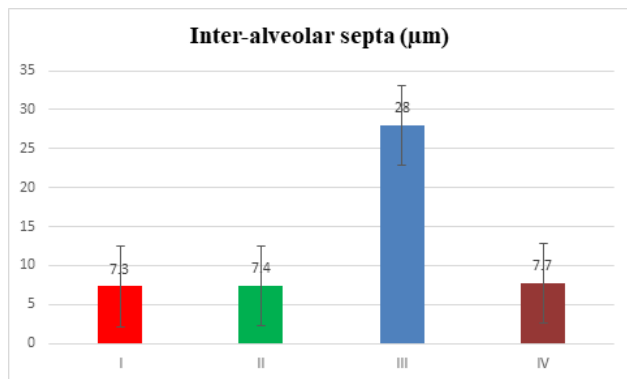
Histogram 3b: Mean values of optical density for iNOS in different groups



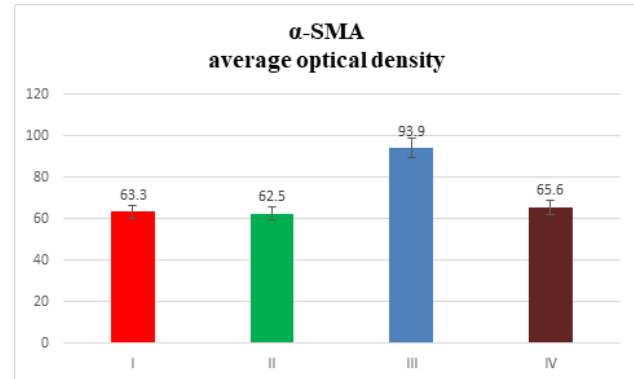
Histogram 2a: Mean values of type II pneumocytes number in different groups



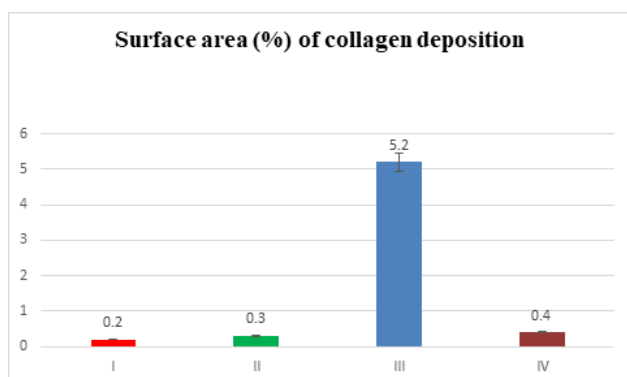
Histogram 3c: Mean values of optical density for caspase-3 in different groups



Histogram 2b: Mean values of inter-alveolar septa in different groups



Histogram 3d: Mean values of optical density for α-SMA in different groups



Histogram 3a: Mean surface area (%) in different groups

DISCUSSION

This current study was undertaken to estimate the potential role of N- acetylcysteine on the lung injury resulting from the administration of Bosutinib. The present work revealed different morphological changes in the specimens taken from rats treated by bosutinib. These changes were in the form of thick inter-alveolar septa and collapsed alveoli, disrupted bronchiolar epithelium with cellular debris in their lumen, congested thickened blood vessels with extravasation of RBCs, increased peri-bronchiolar and perivascular collagen deposition and inflammatory cellular infiltration in the interstitium.

This was in agreement with the findings of Maajid *et al*, 2011^[6] who found chronic interstitial pneumonitis, interstitial fibrosis and cellular infiltration with marked pulmonary vascular thickening after the use of TKI imatinib. In agreement with the present results, Moslehi and Deininger, 2015^[26] who reported that TKIs are related to cardiopulmonary toxicity which could cause morbidity and even mortality.

The mechanism of bosutinib-related lung complications, could be due to oxidative stress (OR) which is responsible for endothelial and pulmonary epithelial apoptosis resulting in an inflammatory environment^[27]. In addition, Christophe *et al*, 2016^[28] showed that TKIs prompts apoptosis in cultured pulmonary endothelial cells via production of mitochondrial reactive oxygen species (ROS) and they observed the significant increase in the apoptotic cells by assessment of Caspase-3/7 activity.

The obvious thickening of inter-alveolar septa in our experiment might be interpreted by the presence of excess inflammatory cells, extravasated RBCs and congested capillaries^[29]. The increase in inflammatory cellular infiltration in the lung was due to the macrophages activation which synthesize interleukin-8 (a potent neutrophil chemotactic) and other inflammatory cells activation. This leads to a rise in their number in interstitium and the vascular space^[30].

Another observation was the presence of homogenous acidophilic material within the inter-alveolar septa and alveoli. Hafez, 2012^[31] found similar results and explained this material as plasma exudates produced as a result of damage of cell wall of the blood vessels. Moreover, Issa and El-sheriff, 2015^[32] reported that the presence of this acidophilic exudates may be due to increased permeability of the alveolar capillary barrier that permits leakage of protein-rich fluid into the septa. Consistent with this finding, TKIs alter endothelial integrity, leading to increased permeability of pulmonary vascular endothelium and fluid leak^[33]. However, Dalvi *et al*, 2014^[34] explained that increased endothelial permeability is ROS dependent mechanism.

Increase the number of types II pneumocytes was detected in our study. This was in agreement with Hinata *et al*, 2003^[35] who stated that proliferation may occur to regenerate the injured type I alveolar epithelium. Moreover, excess ROS production by bosutinib acts as a second messenger to stimulate cell proliferation^[36]. Type II pneumocytes are considered as a local progenitor cells when the alveolar epithelium is damaged, they start proliferation to differentiate into type I pneumocytes to re-establish a functional alveolar epithelium^[37].

As regard of collagen fibers, Mallory trichrome stained sections of bosutinib treated rats, demonstrated marked increase of collagen deposition around the wall of the blood vessels and bronchioles. This was in accordance with Wynn, 2011^[38] who suggested that the mechanism of fibrosis may be due to stimulation of neutrophils and

macrophages to form a various cytokines which amplify the inflammatory response and stimulate proliferation of fibroblast. Once fibroblasts activated, they transformed to myofibroblasts which secrete collagen. The increase in the amount of collagen fibers within the lung interstitium is attributed to the increase in septal thickness^[39]. It has been found that bosutinib administration causes an inflammatory alveolitis with damage to the alveolar epithelium. Alveolar epithelium damage may be induced by ROS, or inflammatory mediators, leading to fibrosis^[40].

For further understanding the mechanism of damage, immune-histochemical study was done using activated Caspase-3 antibody. There was negative immune expression in control rats. This was in accordance with Hafez, 2012^[31] who reported that lung sections stained for caspase-3 revealed no immune reaction of control group. However, obvious cytoplasmic positive caspase-3 immune expression in the epithelium lining alveoli and in the cells scattered in the inter-alveolar septa was observed in bosutinib treated rats. These results could be explained by Hickey *et al*, 2016^[29] who reported that pulmonary cellular damage caused by oxidative stress as a result of bosutinib treatment can induce apoptosis. These apoptotic cells and the abundant cellular debris showed strong immune-expression for caspase-3^[31].

The present work revealed a highly significant increase in the MDA level (a marker of lipid peroxidation) and a significant decrease in the levels of GSH and SOD (antioxidant enzymes) in the lung of bosutinib-treated animals in comparison with the animals of control groups, confirming that bosutinib-induced oxidative stress. TKIs are known to covalently bind GSH resulting in a marked increase in ROS production and reduction of the cellular content of GSH. This goes in line with Xue *et al*, 2012^[41] who found that TKIs reduced the cellular content of the major intracellular antioxidant defense glutathione (GSH) and induced a marked increase in the level of ROS in rat hepatocytes. Parallel to our results, Phan *et al*, 2018^[33] have shown increased levels of lipid peroxidation in lung homogenates of rats treated with high doses of dasatinib. ROS and oxidative stress are responsible for cell-cell junction disruption. In addition, the overproduction of ROS would break down the balance between the oxidative and antioxidative system in the lung, resulting in apoptosis of pulmonary parenchyma^[42].

Regarding the iNOS immunohistochemical staining, there was negative immune expression in the control lung and this agree with Cox *et al*, 2009^[43] who showed similar results. While expression in the bosutinib treated group was significantly increased. This could be explained by Liu *et al*, 2016^[44] who showed that iNOS induced by a variety of proinflammatory cytokines and expressed by activated macrophages. So, when lung exposed to oxidative stress, nitric oxide (NO) reacts with the superoxide free radicals leading to lipid peroxidation in cell membranes^[45].

α -SMA was used as a marker for activated and differentiated myofibroblasts. It is a key mediator during morphological or reparative fibrotic processes^[46]. Group III (Bosutinib treated group) revealed markedly increased expression for α -SMA in the blood vessel, bronchial tree and in the inter-alveolar septa. The precise origin of myofibroblasts is not definite.

It has been suggested that type II pneumocytes might be a source of the myofibroblasts through an epithelial–mesenchymal transition^[47]. Activation of local fibroblasts could be the source of myofibroblasts at the site of fibrosis. However, smooth muscle cells, epithelial cells, endothelial cells pericytes, mesenchymal stem cells and bone marrow-derived cells are other sources of myofibroblasts^[48]. In addition, it has been reported that in the presence of persistent interstitial lung disease caused by TKIs, activated TGF- β 1 can lead to enhanced epithelial apoptosis and epithelial-to-mesenchymal transition as well as fibroblast and fibrocyte, transformation into myofibroblasts which are resistant to apoptosis leading to pulmonary fibrosis^[49]. Studies have shown that acute lung tissue injury and inflammation are major causes for activation and recruitment of bone marrow derived-mesenchymal stem cells to migrate to injured lung and contributed to increase in α -SMA expression^[50].

Co-administration of NAC to bosutinib- treated rats, however, showed a marked decrease in lung morphological changes. Light and electron microscopic examination of group IV revealed a nearly normal lung architecture. Decreased fibrosis was confirmed by a little collagen fiber around the wall of both the bronchiole and blood vessel. Immunostained sections showed decreased expression of both iNOS, Caspase -3 and α -SMA. These results agree with findings of Phan *et al*, 2018^[33] who reported that reduction of dasatinib ROS production by NAC can prevent the increased permeability of pulmonary endothelium *in vitro* and the pleural effusion development in rats. NAC protects the lungs by increasing pulmonary defense mechanisms against toxic agents via its direct antioxidant characteristic and indirect function as a precursor in glutathione formation^[51].

In the present study, there was a more significant decrease in MDA level and a more considerable rise in the level of SOD and GSH after administration of NAC to rats of group IV. In harmony with these findings, several studies reported that NAC supports the synthesis of glutathione (GSH) when the demand for GSH is increased as during oxidative stress. GSH is a critical molecule in resisting oxidative stress^[52]. Oral NAC increases GSH levels by providing the liver with an increased supply of cysteine promoting an increase in GSH synthesis and therefore reduce the oxidative stress^[53]. Previous studies also reported that NAC increased the SOD level and activity in lung injury^[54]. Moreover,^[55] stated that NAC has a direct effect through a free thiol group interacting with and scavenging ROS.

Beside the antioxidant activity of NAC, it has also anti-inflammatory action. This was proved by another research

which revealed strong inhibition of NAC to TNF- α , IL-6, IL-8 in type II pneumocytes infected with influenza virus. NAC also inhibited NF- κ B activation in alveolar macrophages induced by TNF- α ^[56].

From the previous data and results, it can be concluded that administration of NAC has beneficial and protective effects on histological alterations in the lung due to administration of bosutinib. The pulmonary protective effect of NAC seemed to be mediated through its antioxidant and anti-inflammatory activities. So, the study supports the use of NAC as a protective approach against the lung toxicity of bosutinib. More trials on combination of bosutinib with N-acetylcysteine could be discussed in patients of chronic myeloid leukemia or any patient on TKIs.

CONFLICT OF INTERESTS

There are no conflicts of interest.

REFERENCES

1. Jiao Q, Bi L, Ren Y, Song S, Wang Q and Yun-shan W (2018): Advances in studies of tyrosine kinase inhibitors and their acquired resistance. *Molecular Cancer* 17:36.
2. Bagnato G, Leopizzi M, Urciuoli E, Peruzzi B (2020): Nuclear Functions of the Tyrosine Kinase SrcInt. *J. Mol. Sci.*; 21(8): 2675-2689.
3. Metibemu DS, Akinloye OA, Akamo AJ, AjiboyeOjo DO, Okeowo T, Omotuyi O (2019): Exploring receptor tyrosine kinases inhibitors in Cancer treatments *Egyptian Journal of Medical Human Genetics* 20:35.
4. Jain, P, Kantarjian H, Cortes J (2013). Chronic myeloid leukemia: Overview of new agents and comparative analysis. *Current Treatment Options in Oncology*, 14(2), 127–143.
5. O'Brien S, Radich JP, Abboud CN, *et al* (2014): Chronic myelogenous leukemia, version 1.2015. *J Natl Compr CancNetw* 2014; 12: 1590–1610.
6. Maajid M P, Timothy P S, Hamed A D (2011): Pulmonary Toxicities of Tyrosine Kinase Inhibitors. *Clinical Advances in Hematology & Oncology* Volume 9, Issue 11; 824- 836.
7. Boschelli F, Arndt K, Gambacorti-Passerini C (2010): Bosutinib: a review of preclinical studies in chronic myelogenous leukemia. *Eur J Cancer* ;46:1781–1790.
8. Cortes JE, Kantarjian HM, Brümmendorf TH, *et al* (2011): Safety and efficacy of bosutinib (SKI-606) in chronic phase Philadelphia chromosome-positive chronic myeloid leukemia patients with resistance or intolerance to imatinib. *Blood*; 118: 4567–4576.
9. Kantarjian HM, Cortes JE, Kim DW, *et al* (2014): Bosutinib safety and management of toxicity in leukemia patients with resistance or intolerance to imatinib and other tyrosine kinase inhibitors. *Blood*.;123(9):1309–18.

10. Riou M, Seferian A, Savale L, Marie-Camille C, Guignabert C, Canuet M (2016): Deterioration of pulmonary hypertension and pleural effusion with bosutinib following dasatinib lung toxicity. *Eur Respir J*; 48: 1517–1519.
11. Lai KY, Ng WY, Osburga Chan PK, *et al* (2010): High-dose N-acetylcysteine therapy for novel H1N1 influenza pneumonia. *Ann Intern Med*; 152 (10):687–688
12. Sanguinetti CM (2016): N-acetylcysteine in COPD: why, how, and when? *Multidisciplinary Respiratory Medicine* 11:8.
13. Wang AL, Wang JP, Wang H, Chen YH, Zhao L, Wang LS, Wei W, Xu DX (2006): "A dual effect of N-acetylcysteine on acute ethanol-induced liver damage in mice". *Hepatology Research*. 34 (3):19906.
14. Samuni Y, Goldstein S, Dean OM, Berk M (2013): "The chemistry and biological activities of N-acetylcysteine". *Biochimica et Biophysica Acta (BBA) - General Subjects*. 1830 (8): 4117–4129.
15. De Flora S, Balansky R, La Maestra S (2020): Rationale for the use of N-acetylcysteine in both prevention and adjuvant therapy of COVID-19. *The FASEB Journal*.;34:13185–13193.
16. Sevgi E, Semsı A, Serpil B, Erol C (2008): The effect of N-acetylcysteine on brain tissue of rats fed with high-cholesterol diet. *Turk J Biochem*; 33:58-63.
17. Heyen JR, Hu W, Jamieson J, Thibault S, Batugo M, Cho-Ming L (2013): Cardiovascular differentiation of imatinib and bosutinib in the rat *International Journal of Hematology* volume 98, pages597–607.
18. El-Akabawy G and El-Kholy W. (2014): Neuroprotective effect of gigar in the brain of streptozotocin-induced diabetic rats. *Ann Anat*. 169(2):119-128.
19. Del Rio D, Stewart AJ, Pellegrini N. (2005): A review of recent studies on malondialdehyde as toxic molecule and biological marker of oxidative stress. *NutrMetab Cardiovasc Dis*. 15(4):316-328.
20. Saenz-de-Viteri M, Heras-Mulero H, Fernández-Robredo P, *et al* (2014): Oxidative stress and histological changes in a model of retinal phototoxicity in rabbits. *Oxid. Med, Cell Longev*. ;ID 637137.
21. Gloria E, Borgstahl O, Rebecca E (2018). Superoxide Dismutases (SODs) and SOD Mimetics. *Antioxidants*, 7(11): 156- 158.
22. Suvarna K, Layton C, Bancroft J (2013): *Theory and Practice of Histological Techniques*, seventh ed. Churchill Livingstone of Elsevier, Philadelphia, USA, pp.173–214.
23. Dykstra K, Michael J, Laura E (2003): Biological Electron Microscopy Theory, Techniques, and Troubleshooting effect of vitamin E and vitamin C. *Pest Biochem Physiol*. 118:10–18.
24. Sabry MM, Elkalawy SAE, Abo-Elnour RKD (2014): Histological and immunohistochemical study on the effect of stem cell therapy on bleomycin induced pulmonary fibrosis in albino rat. *Int J Stem Cells*. 7(1): 33–42.
25. Peat J and Barton B (2005): *Medical statistics. A Guide to data analysis and critical appraisal*. First Edition. Wiley-Blackwell:113-119.
26. Moslehi JJ, Deininger M (2015): Tyrosine kinase inhibitor-associated cardiovascular toxicity in chronic myeloid leukemia. *J Clin Oncol*; 33: 4210–4218.
27. Jutant EM, Meignin V, Montani D (2017): Bosutinib-related pneumonitis. *Eur Respir J*; 50: 1700930.
28. Christophe G, Carole P, Andrei S, Alice H, Ly T, Raphaël T *et al* (2016): Dasatinib induces lung vascular toxicity and predisposes to pulmonary hypertension. *J Clin Invest*. 126(9): 3207–3218.
29. Hickey PM, Thompson AA, Charalampopoulos A (2016): Bosutinib therapy resulting in severe deterioration of pre-existing pulmonary arterial hypertension. *Eur Respir J*; 48: 1514–1516.
30. Rubin R, Strayer DS, Rubin E (2008): *Rubin's pathology: clinicopathologic foundations of medicine*, 5th ed; 45(2): 283-284. Lippincott Williams and Wilkins.
31. Hafez MS (2012): Effect of selenium supplementation on the structure of the lung of adult albino rats subjected to experimentally induced chronic renal failure. *Egyptian Journal of Histology* ;35(3):573-86.
32. Issa NM, El-sheriff NM (2015): Histological and immunohistochemical study on the toxic effects of Anthracene on the lung and liver of adult male albino rats and the possible protective role of *Ocimum gratissimum* extract. *J Cell Biol Histol*;1:103.
33. Phan C, Jutant EM, Tu L, *et al* (2018): Dasatinib increases endothelial permeability leading to pleural effusion. *Eur Respir J*; 51: 1701096.
34. Dalvi P, Wang K, Mermis J, *et al* (2014): HIV-1/ cocaine induced oxidative stress disrupts tight junction protein-1 in human pulmonary microvascular endothelial cells: role of Ras/ERK1/2 pathway. *PLoS One*; 9 (1): 85246.
35. Hinata N, Takemura T, Lkushima S, Yanagawa T, Ando T, Okada J (2003): Phenotype of regenerative epithelium in idiopathic interstitial pneumonias. *J Med Dent Sci*; 50: 213-224.
36. Brümmendorf TH, Cortes JE, Khoury HJ (2016): Factors influencing long-term efficacy and tolerability of bosutinib in chronic phase chronic myeloid leukaemia resistant or intolerant to imatinib. *Br J Haematol*; 172: 97–110.

37. Anversa P, Kajstura J, Leri A, Loscalzo J (2011): Tissue-specific adult stem cells in the human lung. *Nat. Med.* 17 (9), 1038–1039.
38. Wynn TA (2011): Integrating mechanisms of pulmonary fibrosis. *Journal of Experimental Medicine.*;208(7):1339-50.
39. Wolters PJ, Collard HR, Jones KD (2013): Pathogenesis of idiopathic pulmonary fibrosis. *Ann Rev Pathol*;9: 157-179.
40. Pardo A, Selman M (2002): Idiopathic pulmonary fibrosis: new insights in its patho-genesis. *Int. J. Biochem. Cell Biol.* 34 (12): 1534–1538.
41. Xue T, Luo P, Zhu H, *et al* (2012): Oxidative stress is involved in dasatinib-induced apoptosis in rat primary hepatocytes. *Toxicol Appl Pharmacol*; 261: 280–291.
42. Bergeron A, Rea D, Levy V (2007): Lung abnormalities after dasatinib treatment for chronic myeloid leukemia: a case series. *Am J Respir Crit Care Med*; 176: 814–818.
43. Cox RA, Jacob S, Oliveras G, Murakami K, Enkhbaatar P, Traber L (2009): Pulmonary expression of nitric oxide synthase isoforms in sheep with smoke inhalation and burn injury. *Experimental lung research.*;35(2):104-18.
44. Liu W, Han C, Zhang P, Zheng J, Liu K, Sun X (2016): Nitric oxide and hyperoxic acute lung injury. *Medical gas research*; 6(2):85-92
45. Han ZH, Jiang Y, Duan YY, Wang XY, Huang Y, Fang TZ (2015): Protective effects of hydrogen sulfide inhalation on oxidative stress in rats with cotton smoke inhalation induced lung injury. *Experimental and therapeutic medicine* ;10(1):164-168.
46. Popova AP, Bentley JK, Anyanwu AC, Richardson MN, *et al* (2012): Glycogen synthase kinase-3B/B-catenin signaling regulates neonatal lung mesenchymal stromal cell myofibroblastic differentiation. *Am. J. Physiol. Lung Cell. Mol. Physiol.* 303(5), L439–L448.
47. Kalluri R, Neilson EG (2003): Epithelial–mesenchymal transition and its implications for fibrosis. *J. Clin. Invest.* 112 (12), 1776–1784.
48. Hinz B (2010): The myofibroblast in connective tissue repair and regeneration. In: Ralphs, C.A.J. (Ed.), *Regenerative Medicine and Biomaterials for the Repair of Connective Tissues*. Woodhead Publishing Ltd., Cambridge, UK, pp. 39–82.
49. Coward WR, Saini G, Jenkins G (2010): The pathogenesis of idiopathic pulmonary fibrosis. *Ther. Adv. Respir. Dis.* 4 (6), 367–388.
50. Tang N, Zhao Y, Feng R, Liu Y, Wang S, Wei W, Ding Q, An MS, Wen J, Li L (2014): Lysophosphatidic acid accelerates lung fibrosis by inducing differentiation of mesenchymal stem cells into myofibroblasts. *J. Cell. Mol. Med.* 18 (1),156–169.
51. Dekhuijzen PNR (2004): Antioxidant properties of N-acetylcysteine: their relevance in relation to chronic obstructive pulmonary disease. *Eur Respir J*; 23: 629–636.
52. Zhang, Ju Y, Ma Y, Wang T (2018): N-acetylcysteine improves oxidative stress and inflammatory response in patients with community acquired pneumonia. A randomized controlled trial. *Medicine: Volume 97 - Issue 45 - p e13087*.
53. Soo LO, Ruth G, SokCheon P (2018): N-Acetylcysteine for the Treatment of Psychiatric Disorders: A Review of Current Evidence. *BioMed Research International* 6: 1-8.
54. Nagata K, Iwasaki Y, Yamada T, *et al* (2007): Overexpression of manganese superoxide dismutase by N-acetylcysteine in hyperoxic lung injury. *Respir Med*;101:800–807.
55. Rachel R, Sarah F, Stuart G, Steve R, Philippa A, Adam S, Rosi P, Bronwen J (2018): Assessment of N-acetylcysteine as a therapy for phosgene-induced acute lung injury. *Toxicology Letters*; 290:145–152.
56. De Backer J, Vos W, Van Holsbeke C (2013): Effect of high-dose N-acetylcysteine on airway geometry, inflammation, and oxidative stress in COPD patients. *Int J Chron Obstruct PulmonDis*;8:569–579.

الملخص العربي

دراسة هستولوجيه وهستوكيميائية على تأثير بوسوتينيب على رئة ذكور الفئران البيضاء البالغة والتأثير التحسني المحتمل ن- استيل سيستايين

اميره فهمى على السيد وناديه سعيد بدوى خير

قسم الهستولوجى - كلية الطب - جامعة المنوفية - مصر

المقدمه: ينتمي بوسوتينيب إلى فئة من الأدوية تسمى مثبطات التيروسين كينيز ويستخدم لعلاج نوع معين من سرطان الدم النخاعي المزمن. إنه يعمل عن طريق منع عمل البروتين غير الطبيعي الذي يؤدي إلى تكاثر الخلايا السرطانية. إعطاء البوسوتينيب يؤدي إلى بعض المضاعفات التنفسية . ن- استيل سيستايين , هو دواء يستخدم لعلاج حالات مثل التليف الكيسي والربو, كما انه منتج ثانوي للجلوتاثيون .

الهدف من البحث: تهدف هذه الدراسة لتقييم تأثير بوسوتينيب على رئة ذكور الجرذان البيضاء البالغة والتأثير الوقائي المحتمل لـ ن- استيل سيستايين.

الطرق المستخدمه : أجريت هذه الدراسة على ثمانية و أربعين من ذكور الجرذان البيضاء. تم تقسيمهم إلى أربع مجموعات ، المجموعة الأولى (المجموعة الضابطة) ، المجموعة الثانية (المجموعة المعالجة ب ن- استيل سيستايين)، المجموعة الثالثة (المجموعة المعالجة بالبوسوتينيب)، والمجموعة الرابعة (المجموعة المعالجة بالبوسوتينيب و ن- استيل سيستايين). في نهاية التجربة ، تمت معالجة أنسجة الرئة للدراسات النسيجية والمناعية

النتائج: أظهر الفحص بان المجموعة المعالجة بالبوسوتينيب تظهر تغيرات نسيجية بدرجات متفاوتة على رئة الحيوانات , بعض الحويصلات الهوائية ضيقه مع وجود ترسب مادة هيالين في البعض الآخر ، وكانت مبطنة بشكل أساسي بالخلايا الرئوية من النوع الثاني , مع زياده سمك الحواجز بين الحويصلات . كما لوحظ ارتشاح خلوي واحتقان في الأوعية الدموية مع تليف حول الأوعية الدموية. كما اظهر الفحص بالمجهر الالكتروني عن حدوث تغيرات في الخلايا الرئوية من النوع الأول والنوع الثاني. كانت هذه التغييرات أقل وضوحًا في المجموعة المعالجة بالبوسوتينيب و ن- استيل سيستايين.

الخلاصة: بوسوتينيب له تأثير سام على أنسجة الرئة يمكن تحسينه عن طريق تناول المتزامن لـ ن- استيل سيستايين